Research Square

Preprints are preliminary reports that have not undergone peer review.
They should not be considered conclusive, used to inform clinical practice,
or referenced by the media as validated information.

Application of Magnetic Susceptibility and Heavy-Metal Concentrations to Assess Soil Pollution Around Savannah Sugar Company, Numan, Adamawa State, Nigeria

Nsisong Joseph Obot

nsisongjosephjohnobot@gmail.com

Taraba State University

Maxwell O. Kanu

Taraba State University

Research Article

Keywords: Magnetic susceptibility, Heavy metals, Soil pollution, Pollution indices, Ecological risk, Human-health risk, Agro-industrial soil

Posted Date: November 5th, 2026

DOI: https://doi.org/10.21203/rs.3.rs-11365338/v1

License: This work is licensed under a Creative Commons Attribution 4.0 International License.
Read Full License

Additional Declarations: No competing interests reported.

Application of Magnetic Susceptibility and Heavy-Metal Concentrations to Assess Soil Pollution Around Savannah Sugar Company, Numan, Adamawa State, Nigeria

Nsisong Joseph Obot[1], Maxwell O. Kanu[1]*
[1]Department of Physics, Taraba State University, Jalingo, Taraba State, Nigeria.
Authors' Email Addresses:
Nsisong Joseph Obot: nsisongjosephjohnobot@gmail.com
Corresponding Author: Maxwell O. Kanu
Corresponding Author's Email: Maxwell.kanu@tsuniversity.edu.ng

Abstract

Agro-industrial activities may contribute to heavy-metal accumulation in surrounding soils, creating potential ecological and human-health risks. This study assessed soil pollution around the Savannah Sugar Company (SSC), Numan, Adamawa State, Nigeria, using magnetic susceptibility, X-ray fluorescence (XRF), scanning electron microscopy with energy-dispersive spectroscopy (SEM–EDS), pollution indices, multivariate statistics and human-health risk assessment. A total of 200 soil samples comprising topsoil, farmland-reference, vertical-profile and lateral-transect samples were analysed for low- and high-frequency magnetic susceptibility (χLF and χHF), while 30 selected samples were analysed by XRF for eleven elements. Topsoil χLF ranged from 21 to 1,473 × 10^{-8} m^3 kg^{-1}, while lateral-transect χLF ranged from 24 to 486 × 10^{-8} m^3 kg^{-1}, indicating marked spatial magnetic variability. Pb, Co, Cu and Ni showed substantial enrichment, with Pb reaching 1,350 mg kg^{-1}. The Pollution Load Index exceeded unity in all analysed samples (mean = 4.83), while the Potential Ecological Risk Index ranged from 199.9 to 547.5 (mean = 349.3), with 60% of samples classified as considerable risk. Pearson correlation analysis (n = 29) showed significant positive relationships between χLF and Fe ($r = 0.584$, $p < 0.01$), Mn ($r = 0.558$, $p < 0.01$) and Ti ($r = 0.427$, $p < 0.05$), indicating that magnetic susceptibility may provide a useful preliminary screening indicator of Fe-, Mn- and Ti-associated enrichment. Multivariate and SEM–EDS analyses indicated mixed geogenic/pedogenic and anthropogenic influences. Human-health assessment showed that the adult Hazard Index remained below unity, whereas the child Hazard Index exceeded unity, driven mainly by chromium. The findings demonstrate substantial multi-metal contamination around the SSC and support combining magnetic screening with direct geochemical analysis for environmental monitoring.

Keywords: Magnetic susceptibility; Heavy metals; Soil pollution; Pollution indices; Ecological risk; Human-health risk; Agro-industrial soil.

1. Introduction

Soil contamination by heavy metals has become one of the more persistent environmental problems accompanying industrialisation and agricultural intensification in the developing world. Metals such as lead, cadmium, chromium, copper, nickel and cobalt are non-biodegradable, bioaccumulate along food chains, and remain toxic to soil biota and human health even at trace concentrations (Tchounwou et al., 2012; Balali-Mood et al., 2021). Once introduced into the topsoil through industrial effluent, atmospheric deposition, fertiliser use or vehicular traffic, these elements degrade soil fertility, disrupt microbial and nutrient cycling, and create a long-lived exposure pathway for surrounding communities through ingestion,

dermal contact and inhalation of soil dust (Alengebawy et al., 2021; Das et al., 2023; Oloruntoba et al., 2024).

Conventional assessment of soil metal contamination relies on wet-chemical or spectrometric analysis, which, although accurate, is costly and time-consuming, limiting the frequency and spatial density of monitoring that can realistically be sustained in many African settings. Environmental magnetism offers a complementary, low-cost alternative: soil magnetic susceptibility (χ) responds to the concentration of ferrimagnetic minerals, which are frequently co-emitted with metal-bearing particulates from combustion, vehicular and industrial sources, so that χ can act as a rapid proxy for metal enrichment (Thompson & Oldfield, 1986; Dearing et al., 1996). Several Nigerian studies have reported strong positive correlations between soil χ and metal concentrations at automobile and industrial sites (Orosun et al., 2020; Kanu et al., 2022), lending support to its use as a first-pass screening tool ahead of more expensive geochemical surveys.

Beyond raw concentrations, a suite of indices has been developed to translate metal data into interpretable measures of contamination severity and ecological or human risk. The Contamination Factor (CF) and Pollution Load Index (PLI) express metal enrichment relative to a geochemical background (Tomlinson et al., 1980), the Geoaccumulation Index (Igeo) applies a logarithmic classification originally developed for sediments, and the Potential Ecological Risk Index (RI) weights contamination by each metal's relative toxicity (Hakanson, 1980). Human exposure is separately quantified through the Chronic Daily Intake, Hazard Quotient/Index and Cancer Risk framework recommended by the United States Environmental Protection Agency, which converts measured soil concentrations into estimates of non-carcinogenic and carcinogenic risk for defined exposure scenarios (USEPA, 2011).

The Savannah Sugar Company (SSC) estate near Numan, Adamawa State, north-eastern Nigeria, is a large agro-industrial complex whose sugarcane fields and processing plant are irrigated from the Kiri Dam and lie immediately adjacent to the residential settlements of Gyawana and Boshikiri. Activities associated with sugarcane cultivation and sugar processing at the Savannah Sugar Company provide several potential pathways for the enrichment of magnetic particles and heavy metals in surrounding soils. Agricultural activities within the estate involve the application of fertilisers and agrochemicals, irrigation, movement of farm machinery and repeated vehicular traffic, while industrial operations associated with sugar processing include bagasse combustion for steam and power generation, handling of processing wastes and the discharge or movement of wastewater through drainage and irrigation channels. Combustion processes can generate ash and fine ferrimagnetic particulates containing iron-bearing minerals, which may be deposited on nearby soils and consequently increase their magnetic susceptibility. Similarly, agrochemical application, industrial waste or effluent, ash deposition, machinery wear and vehicular emissions may introduce or redistribute metals such as Cr, Co, Ni, Cu, Zn and Pb in surface soils. The combined influence of these agricultural and industrial activities therefore provides plausible mechanisms for both magnetic enhancement and heavy-metal accumulation within and around the SSC. Maitera et al. (2023) previously reported elevated iron, zinc, lead, cadmium and manganese in soils around the SSC, with cadmium concentrations exceeding World Health Organization limits, and explicitly called for

further investigation using complementary techniques to better characterize contamination sources and risks in the area. To date, however, no published study has combined magnetic susceptibility measurement with multi-element geochemistry, particle-level morphological evidence, pollution indices and quantitative health-risk modelling for this site, leaving both the extent of contamination and its likely sources poorly constrained.

The present study addresses this gap by (i) quantifying the concentrations of eleven elements (Ti, V, Cr, Mn, Fe, Co, Ni, Cu, Zn, Rb, Pb) in soils around the SSC; (ii) measuring bulk soil magnetic susceptibility across a spatially extensive sampling network that includes vertical depth profiles and lateral distance transects; (iii) testing whether magnetic susceptibility can serve as a statistical proxy for metal enrichment; (iv) evaluating the degree of soil pollution and ecological risk using established indices; and (v) estimating the non-carcinogenic and carcinogenic health risks to which nearby residents may be exposed through incidental soil ingestion.

2. Materials and Methods

2.1 Study area

The study was conducted around the Savannah Sugar Company (SSC) estate in Numan Local Government Area, Adamawa State, Nigeria. The study area is geographically located around latitude 9°35.398′ N and longitude 11°54.707′ E, as shown in Figure 1. The SSC occupies approximately 32,000 ha northeast of Numan town and is irrigated by canals drawing water from the Kiri Dam, approximately 12 km upstream. The settlements of Gyawana and Boshikiri are located adjacent to the sugarcane fields, with agricultural and residential land uses occurring alongside the industrial estate. The area experiences a tropical wet dry climate, with rainfall concentrated between April and October and a pronounced dry season from November to March. Soils in the Numan area have been described by Zata et al. (2013) as predominantly clayey Vertisols characterised by pronounced shrink–swell behaviour associated with alternating wet and dry conditions. The Numan Vertisols occur mainly on relatively level terrain and are associated with alluvial deposits in the area.

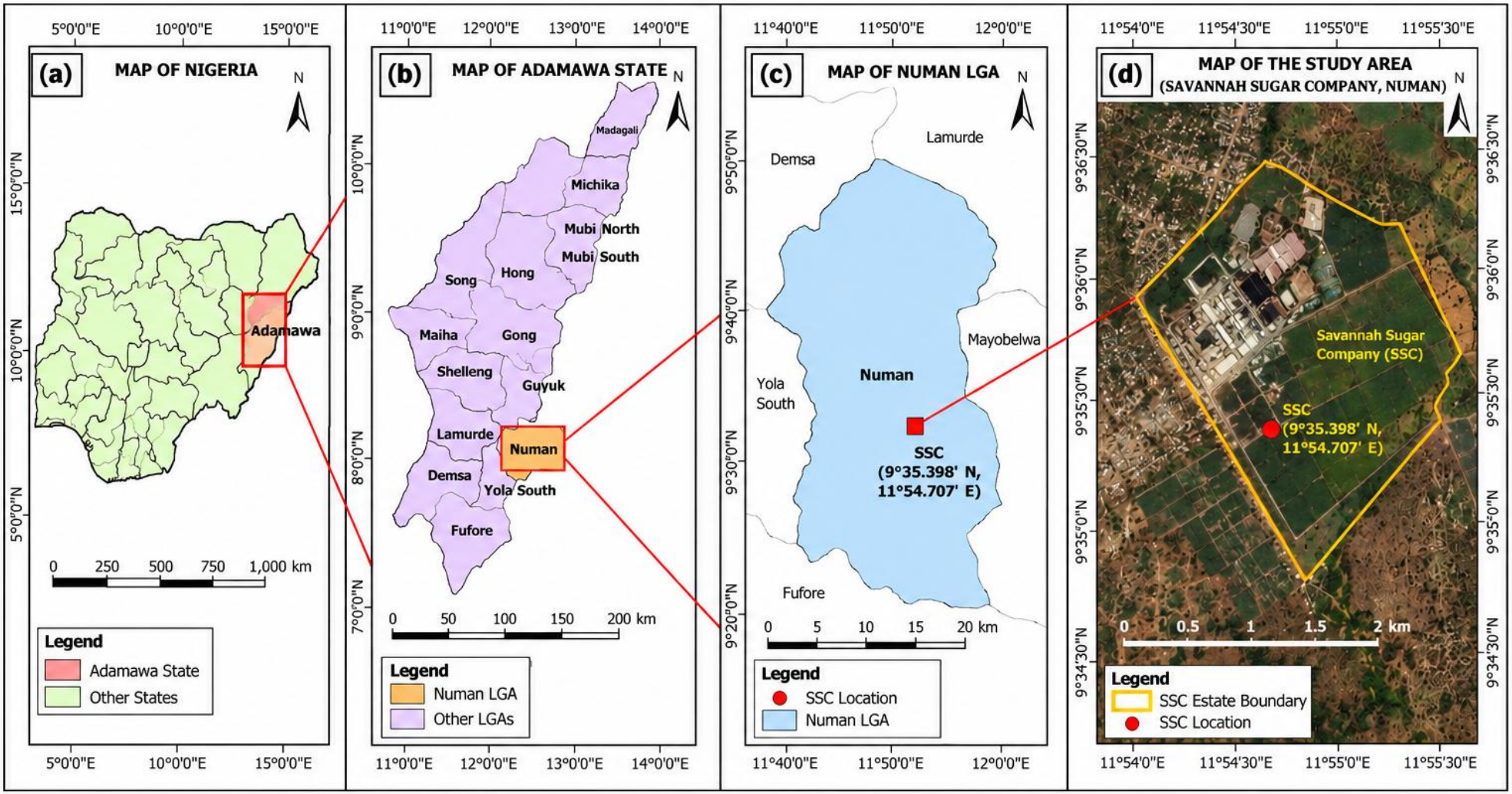


Fig. 1. Location of the study area: (a) Nigeria, showing Adamawa State; (b) Adamawa State, showing Numan Local Government Area; (c) Numan LGA, showing the study area relative to the River Benue floodplain; (d) satellite view of the Savannah Sugar Company estate and sampling area boundary.

2.2 Soil sampling

A total of 200 samples (0–20 cm) were collected using a hand auger and geo-referenced with a handheld GPS (Garmin 12) receiver. The sampling design comprised four components: (i) 70 topsoil stations (TS1–TS70) randomly collected across the industrial and residential strata of the study area; (ii) Twenty-four samples (FATS1–FATS24) were collected from farmland adjacent to the staff quarters and relatively distant from the main industrial and residential zones. (iii) six vertical soil profiles (AVP–FVP), each sampled at 5 cm intervals from 0 to 50 cm depth (11 samples per profile, 66 samples in total) to investigate depth-related magnetic susceptibility stratification; and (iv) four lateral transects (CTS, DTS, ETS, FTS) radiating from the four sides of the sugar-processing plant, each sampled at ten fixed distances between 2 and 50 m (40 samples in total) to examine variations of magnetic susceptibility with distance away from the pollution source. All samples were air-dried, disaggregated with a mortar and pestle, and sieved to < 2 mm prior to laboratory analysis.

2.3 Magnetic susceptibility measurement

Magnetic susceptibility was measured on all 200 samples at the Physics Laboratory, Modibbo Adama University, Yola, Nigeria, using a Bartington MS2 meter fitted with an MS2B dual-frequency sensor (Bartington Instruments Ltd, UK), calibrated against the manufacturer's reference sample (Serial No. 798; 3,121 × 10^{-5} SI). Each sample was weighed and measured at low frequency (χLF, 0.465 kHz) and high frequency (χHF, 4.65 kHz), and mass-specific susceptibility was obtained by dividing the instrument reading by sample mass. Frequency-dependent susceptibility, an indicator of the proportion of ultrafine superparamagnetic grains, was calculated as

$$\chi FD\% = \frac{(\chi LF - \chi HF)}{\chi LF} \times 100 \quad (1)$$

2.4 X-ray fluorescence (XRF) elemental analysis

Thirty topsoil samples were selected for elemental analysis based on their χLF values to represent the observed range of magnetic susceptibility. The selected samples comprised eight with extremely high, seven with high, seven with moderate and eight with low χLF values. Analysis was performed at the National Steel Raw Materials Exploration Agency (NSRMEA), Kaduna State, Nigeria, using a Xenemetrix Genius IF energy-dispersive X-ray fluorescence (ED-XRF) spectrometer (Series EX-2600/X-2600). Pulverised samples were loaded into Prolene-film sample cups and analyzed under standard operating conditions. The resulting spectra were processed using XRS-FP software with the Master Oxide calibration file to determine the concentrations (mg kg^{-1}) of Ti, V, Cr, Mn, Fe, Co, Ni, Cu, Zn, Rb and Pb.

2.5 Scanning electron microscopy (SEM–EDS)

Four samples spanning a representative range of geochemical and magnetic characteristics (TS12, TS13, TS18, TS30) were selected for particle-morphology analysis by scanning electron microscopy at the NSRMEA, using a Phenom ProX benchtop SEM (Phenom-World B.V.). Pulverised material was mounted on aluminium stubs with carbon adhesive tabs and

imaged at 15 kV accelerating voltage and 60 Pa chamber pressure, at magnifications of 320–500×, with selected regions further analysed by energy-dispersive spectroscopy (EDS).

2.6 Pollution and ecological-risk indices

Four complementary indices were computed for the 30 XRF-analysed samples. The Contamination Factor for each metal was calculated as

$$\mathrm{CF} = \frac{Csample}{Cbackground} \quad (2)$$

where Csample is the measured concentration and Cbackground is the regional geochemical background; CF < 1 indicates low, 1–3 moderate, 3–6 considerable, and > 6 high contamination (Hakanson, 1980). The Pollution Load Index, the geometric mean of the CF values across all analysed metals in a sample, was calculated as

$$PLI = (CF1 \times CF2 \times \cdots \times CFn)^{(1/n)} \quad (3)$$

with PLI ≥ 1 indicating pollution relative to background (Tomlinson et al., 1980). The Geoaccumulation Index was calculated as

$$Igeo = log2\,[\frac{Csample}{(1.5 \times Cbackground)}] \quad (4)$$

where the factor 1.5 corrects for natural lithogenic variation in background values; soils are classified from practically uncontaminated (Igeo ≤ 0) through moderately (0–1), moderately-to-strongly (1–2), strongly (2–3), strongly-to-extremely (3–4) and extremely contaminated (Igeo > 5). Ecological risk was evaluated for the six metals with established toxic-response factors (Tr): 5 for Co, Ni, Cu and Pb; 2 for Cr; and 1 for Zn (Hakanson, 1980). The individual ecological risk factor was calculated as Er = Tr × CF, and the overall Potential Ecological Risk Index as

$$\boxed{E_r^i = T_r^i \times CF^i}$$
$$RI = \Sigma\, Er \quad (5)$$

with RI classified as low (< 150), moderate (150–300), considerable (300–600), high (600–1200) or very high (≥ 1200) risk.

2.7 Human-health risk assessment

Non-carcinogenic and carcinogenic risk from incidental soil ingestion were assessed for six metals of toxicological concern (Cr, Co, Ni, Cu, Zn, Pb) following USEPA methodology. The Chronic Daily Intake (CDI, mg kg^{-1} day^{-1}) was calculated as

$$CDI = \frac{(C \times IR \times EF \times ED \times ABF)}{(BW \times AT)} \quad (6)$$

where C is soil metal concentration; IR is the soil ingestion rate (100 mg day^{-1} for adults, 200 mg day^{-1} for children); EF is exposure frequency (350 days $year^{-1}$); ED is exposure duration (24 years for adults, 6 years for children); ABF is the absorption factor (0.14 for Pb, 1 for the

remaining metals); BW is body weight (70 kg adults, 15 kg children); and AT is the averaging time. The Hazard Quotient was calculated as HQ = CDI / RfD, where RfD is the metal's oral reference dose, and the Hazard Index (HI) as the sum of HQ values across the six metals; HI > 1 indicates a potential cumulative non-carcinogenic risk. Cancer Risk (CR) was calculated as CR = CDI × SF for metals with an established oral cancer slope factor (SF): lead, and chromium under the conservative assumption that a fraction of measured total chromium occurs as the carcinogenic Cr (VI) species. CR values below 10^{-6} are considered negligible, 10^{-6}–10^{-4} an acceptable range, and above 10^{-4} potentially unacceptable (USEPA, 2011).

2.8 Statistical analysis

Descriptive statistics (mean, standard deviation, range) were calculated for χ parameters and metal concentrations. Pearson correlation coefficients were computed between χLF and each metal, and among metals, with significance assessed at $p < 0.05$ and $p < 0.01$. Principal Component Analysis (PCA) with Varimax rotation was applied to the standardised dataset (χLF plus 11 elements, n = 29 samples with matched χ and XRF data), retaining components with eigenvalues > 1 (Kaiser criterion). Hierarchical Cluster Analysis (HCA), using Ward's minimum-variance linkage and squared Euclidean distance, was performed independently on the same standardised dataset to cross-validate the PCA-derived source groupings. All statistical analyses were performed in SPSS.

3. Results and Discussion

3.1 Soil magnetic susceptibility

Low-frequency magnetic susceptibility (χLF) across the 70 topsoil stations ranged from 21 to 1,473 × 10^{-8} m^3 kg^{-1}, with a mean of 156.43 ± 191.17 × 10^{-8} m^3 kg^{-1} (Table 1). The single highest value occurred at TS1 (1,473 × 10^{-8} m^3 kg^{-1}), in the inner residential zone closest to the factory complex, while a secondary cluster of elevated values (TS60–TS65: 284–518 × 10^{-8} m^3 kg^{-1}) coincided with the eastern SSC-adjacent zone where effluent canals, factory operations and traffic converge. Farmland topsoil samples had a mean χLF of 104.42 ± 71.49 × 10^{-8} m^3 kg^{-1}, markedly lower than the industrial/residential stations and consistent with a more purely geogenic signal. Frequency-dependent susceptibility (χFD%) averaged 4.8 ± 4.4% (range 0–23.3%), with roughly 90% of samples falling in the 2–10% range typical of a mixed coarse/fine magnetic-grain assemblage; only seven stations exceeded 10%, suggesting that the elevated χLF values across most of the study area are dominated by coarser, largely anthropogenic ferrimagnetic particles rather than fine pedogenic grains (Dearing et al., 1996).

The lateral transect samples (CTS, DTS, ETS and FTS) showed χLF values ranging from 24 to 486 × 10^{-8} m^3 kg^{-1}, with a mean of 153.65 ± 97.19 × 10^{-8} m^3 kg^{-1}. The corresponding χHF values ranged from 22 to 343 × 10^{-8} m^3 kg^{-1}, with a mean of 131.65 ± 75.53 × 10^{-8} m^3 kg^{-1}. Frequency-dependent susceptibility (χFD%) ranged from 0.00 to 41.04%, with a mean of 4.58 ± 6.40%. The maximum χLF value (486 × 10^{-8} m^3 kg^{-1}) occurred along ETS at 20 m, whereas the highest χFD% (41.04%) occurred along DTS at 20 m. The marked variability among the

transects indicates spatial heterogeneity in the concentration and grain-size distribution of magnetic minerals around the processing plant.

Vertical profiling revealed marked sub-surface anomalies. Profile CVP recorded the highest values of any profile, peaking at 617 and 819 × 10^{-8} m^3 kg^{-1} at 20 and 25 cm depth respectively, with correspondingly low χFD% (0.98–5.7%), indicating a buried layer of coarse magnetic material, plausibly historical ash or slag deposition. Profiles EVP and FVP, by contrast, remained uniformly low (13–28 × 10^{-8} m^3 kg^{-1}) throughout, representing background conditions away from direct industrial influence. The lateral transects showed substantial spatial variability rather than a consistent monotonic decline in χLF with increasing distance from the processing plant, suggesting localised controls on the distribution of magnetic particles. The pronounced subsurface maximum in CVP, together with low χFD%, is consistent with a discrete layer enriched in coarse ferrimagnetic material rather than purely pedogenic ultrafine grains. The overall magnetic pattern therefore points to a mixed geogenic–anthropogenic control, with local enhancement near industrial, traffic and drainage corridors. Comparable Nigerian studies have reported magnetic enhancement in soils affected by automobile and industrial activities (Orosun et al., 2020; Kanu et al., 2022).

Table 1. Descriptive Statistics of Magnetic Susceptibility Measurements for Soil Samples Around Savannah Sugar Company, Numan

Sample group/Parameter	n	Minimum	Maximum	Mean	SD	CV (%)
Topsoil samples (TS1–TS70)						
χLF (×10^{-8} m^3 kg^{-1})	70	21.00	1473.00	156.43	191.17	122.21
χHF (×10^{-8} m^3 kg^{-1})	70	20.00	1470.00	149.97	190.41	126.96
χFD (%)	70	0.00	23.33	4.75	4.45	93.79
Farmland topsoil (FATS1–FATS24)						
χLF (×10^{-8} m^3 kg^{-1})	24	21.00	255.00	104.42	71.49	68.47
χHF (×10^{-8} m^3 kg^{-1})	24	20.00	241.00	99.88	69.67	69.76
χFD (%)	24	0.62	25.53	5.57	5.19	93.20
Transect samples (CTS, DTS, ETS, FTS)						
χLF (×10^{-8} m^3 kg^{-1})	40	24.00	486.00	**153.65**	**97.19**	**63.25**
χHF (×10^{-8} m^3 kg^{-1})	40	22.00	343.00	**131.65**	**75.53**	**57.37**
χFD (%)	40	0.00	41.04	**4.58**	**6.40**	**139.82**

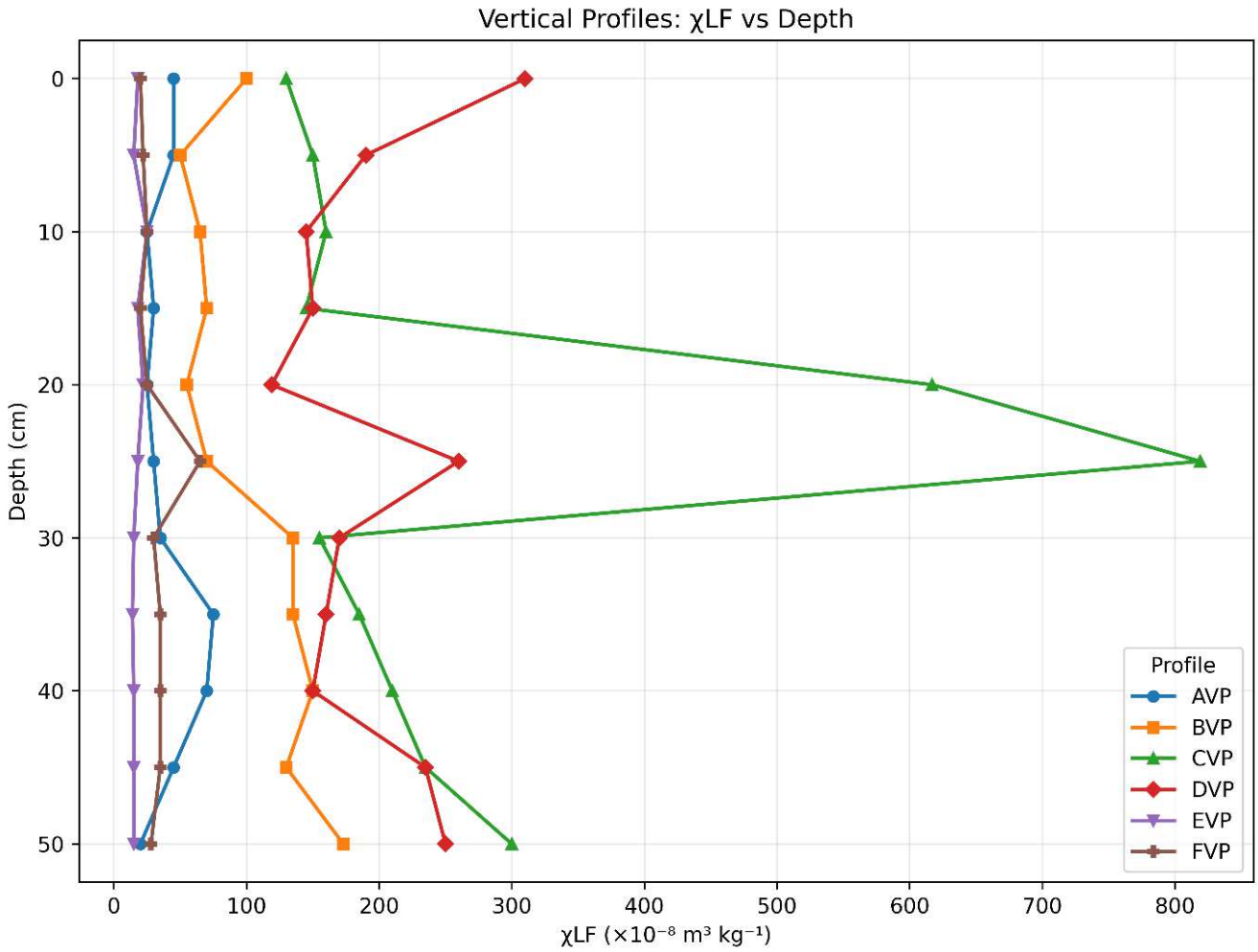


Fig. 2. Variation of low-frequency magnetic susceptibility (χLF) with depth for the six vertical soil profiles (AVP–FVP) around Savannah Sugar Company, Numan.

3.2 Heavy-metal concentrations and contamination pattern

The elemental concentrations of the study-area soils are summarised in Table 2. Iron was the most abundant element (25,510–96,360 mg kg^{-1}; mean 64,332 mg kg^{-1}), while titanium ranged from 6,500 to 14,710 mg kg^{-1} (mean 10,732 mg kg^{-1}). Vanadium, manganese and rubidium broadly followed this geogenic pattern. In contrast, cobalt (40–510 mg kg^{-1}; mean 238.3 mg kg^{-1}), nickel (20–840 mg kg^{-1}; mean 168.3 mg kg^{-1}), copper (210–1,100 mg kg^{-1}; mean 524.3 mg kg^{-1}) and, most notably, lead (190–1,350 mg kg^{-1}; mean 418.0 mg kg^{-1}) showed marked enrichment relative to the adopted background values. Lead reached 1,350 mg kg^{-1} at TS52, equivalent to 67.5 times the background concentration. Nickel and copper both peaked at TS12, whereas zinc displayed the greatest relative variability (30–1,390 mg kg^{-1}). These spatially heterogeneous enrichments indicate that natural lithology alone cannot explain the distribution of the trace metals. The pattern is compatible with superimposed anthropogenic inputs associated with agrochemicals, industrial wastes or effluent, ash deposition, machinery wear and vehicular activity around the SSC. Maitera et al. (2023) similarly reported elevated metals

in soils around the SSC, supporting the interpretation that the estate is affected by agro-industrial contamination.

Table 2. Descriptive Statistics of Elemental Concentrations in Soil Samples Around Savannah Sugar Company, Numan

Element (mg/kg^{-1})	n	Minimum	Maximum	Mean	SD	CV (%)	Kanu et al. (2022) Background	WHO/FAO (2007) Guideline	USEPA (2011) Reference
Ti	30	6,500	14,710	10,732.3	2,422.2	22.57	4,200	N/A	N/A
V	30	260	810	583.7	144.7	24.79	90	N/A	N/A
Cr	30	180	1,010	440.0	176.9	40.20	70	100	210
Mn	30	440	2,290	1,495.7	462.6	30.93	850	2,000	1,800
Fe	30	25,510	96,360	64,332.3	18,254.1	28.37	38,000	N/A	N/A
Co	30	40	510	238.3	116.3	48.80	12	50	23
Ni	30	20	840	168.3	199.0	118.24	35	50	50
Cu	30	210	1,100	524.3	175.5	33.47	30	100	63
Zn	30	30	1,390	256.3	352.1	137.38	95	300	200
Rb	30	110	350	207.7	59.3	28.55	90	N/A	N/A
Pb	30	190	1,350	418.0	262.3	62.75	20	100	70

Table 3: XRF Elemental Concentrations (mg/kg^{-1}) of Selected Soil Samples from the SSC Study Area

Sample	Ti	V	Cr	Mn	Fe	Co	Ni	Cu	Zn	Rb	Pb
TS2	7,120	400	650	1,090	44,240	160	30	730	50	190	440
TS5	11,470	680	420	2,140	96,360	510	70	430	110	280	230
TS7	6,500	260	390	440	25,510	40	200	210	30	110	400
TS8	10,480	650	210	1,560	65,490	340	30	520	90	240	380
TS9	13,620	720	360	2,290	80,720	210	90	540	210	260	370
TS10	11,530	580	530	2,120	88,590	330	160	600	510	250	980
TS11	10,650	540	1,010	1,450	56,440	50	170	610	940	200	270
TS12	9,980	630	380	1,350	81,510	220	840	1,100	500	200	300
TS13	6,750	350	370	1,080	48,160	130	530	310	90	170	230
TS17	10,810	560	510	1,630	68,370	170	80	440	170	240	310
TS18	12,900	610	580	1,550	65,490	210	190	470	80	200	190
TS19	7,600	520	400	770	32,140	320	40	370	70	140	460
TS20	10,130	340	750	1,320	57,260	180	120	780	210	170	460
TS24	12,760	660	540	1,650	71,600	210	110	650	120	260	400
TS30	7,410	500	330	1,010	58,230	440	50	660	30	150	870
TS35	14,710	810	440	1,800	78,020	380	60	430	100	260	200
TS38	10,410	790	230	1,540	65,190	130	120	550	90	140	260
TS39	10,070	430	310	740	37,390	150	20	490	110	180	510
TS40	8,520	520	760	1,740	46,840	380	70	540	60	150	320
TS41	7,980	760	380	1,100	50,300	130	580	270	30	110	240
TS42	8,420	390	340	810	44,880	180	40	610	250	160	280
TS43	14,320	680	180	1,850	82,410	260	80	390	240	250	210
TS44	9,320	620	370	1,250	72,710	200	610	300	110	180	190
TS46	14,190	640	340	2,080	89,690	320	70	700	1,390	300	400
TS48	12,490	680	490	1,970	66,640	220	120	420	80	180	230

TS52	11,420	690	320	1,460	64,770	200	120	460	100	350	1,350
TS56	13,530	630	320	1,950	84,360	240	70	660	1,300	280	370
TS57	10,910	410	410	1,750	47,500	120	90	490	410	270	660
TS63	13,520	710	550	1,670	85,280	460	170	480	130	160	710
TS86	12,450	750	330	1,710	73,880	260	120	520	80	200	320
Minimum	6,500	260	180	440	25,510	40	20	210	30	110	190
Maximum	14,710	810	1,010	2,290	96,360	510	840	1,100	1,390	350	1,350
Mean	10,732.3	583.7	440.0	1,495.7	64,332.3	238.3	168.3	524.3	256.3	207.7	418.0
SD	2,422.2	144.7	176.9	462.6	18,254.1	116.3	199.0	175.5	352.1	59.3	262.3
Background[a]	4,200	90	70	850	38,000	12	35	30	95	90	20

Source: (a) Background values obtained the Nigerian geochemical baseline literature used in the main work (Adamu & Nganje, 2010; Ntekim et al., 2013)

3.3 SEM–EDS particle morphology

Micrographs from the four analysed samples (Fig 2) revealed a heterogeneous particle assemblage. Angular to sub-angular grains consistent with weathered primary silicate minerals (quartz, feldspar, clay) dominated the coarse fraction in all samples, alongside subordinate rounded to sub-rounded grains reflecting alluvial or irrigation-water transport. Sample TS12 was distinguished by porous, spongy particle textures characteristic of fly-ash or combustion-derived material (Fisher et al., 1976), coinciding with the highest Ni (840 mg kg^{-1}) and Cu (1,100 mg kg^{-1}) concentrations recorded in the dataset; given that the SSC operates bagasse-fired boilers for steam and power generation, the observed particle morphology is consistent with a possible contribution from combustion-derived particulates. The fine particulate material observed at TS30, together with its elevated Pb concentration, is consistent with a possible contribution from traffic- or machinery-related sources. This particle-level evidence corroborates the geochemical interpretation that both combustion emissions and vehicular traffic contribute discrete anthropogenic metal inputs superimposed on the geogenic background. The occurrence of irregular and locally spheroidal particles, together with Fe-rich phases and associated trace elements, supports the coexistence of natural mineral grains and combustion- or process-derived particles. Such morphology is consistent with high-temperature particulate formation reported for fly ash (Fisher et al., 1976), although SEM–EDS evidence alone cannot assign a unique source to every particle.

3.4 Pollution indices and their implications

The contamination indices revealed substantial enrichment of several metals in soils around the Savannah Sugar Company. Contamination Factor (CF) values were relatively low for the predominantly lithogenic elements, with mean CF values of 2.56 for Ti, 2.31 for Rb, 1.69 for Fe, and 1.76 for Mn. In contrast, V and Cr showed appreciable enrichment, with mean CF values of 6.49 and 6.29, respectively. The greatest contamination was associated with Pb, Co and Cu. Pb recorded the highest mean CF of 20.90, ranging from 9.50 to 67.50, with the maximum occurring at TS52. Co recorded a mean CF of 19.86 (3.33–42.50), while Cu had a mean CF of 17.48 (7.00–36.67). Ni and Zn showed greater spatial variability, with Zn ranging from 0.32 to 14.63 and particularly high values at TS46 and TS56.

The Pollution Load Index (PLI), calculated as the geometric mean of the CF values of the eleven analysed elements, ranged from 2.38 at TS7 to 7.44 at TS10, with an overall mean of

4.83. All 30 samples recorded PLI values greater than 1, demonstrating multi-element enrichment above the adopted background concentrations throughout the study area. Twenty-four samples (80%) had PLI values above 3, while eight samples (27%) exceeded 5. The highest PLI values occurred at TS10 (7.44), TS12 (7.19), TS46 (6.89), TS56 (6.39), and TS63 (6.09), indicating that the greatest combined metal loads occurred mainly within the residential core and SSC-adjacent locations.

The Geoaccumulation Index (Igeo) showed a similar pattern of metal enrichment. Ti had Igeo values of 0.05–1.22 (mean = 0.73), Fe had a mean of 0.10, Mn 0.24, and Rb ranged from −0.30 to 1.37 (mean = 0.56), indicating relatively low accumulation consistent with a strong lithogenic contribution. V recorded a mean Igeo of 2.10, while Cr ranged from 0.78 to 3.27 (mean = 1.98). The highest accumulation was associated with Pb and Co. Pb ranged from 2.66 to 5.49 (mean = 3.60), reaching its maximum at TS52 (Igeo = 5.49), while Co ranged from 1.15 to 4.82 (mean = 3.53). Cu also showed substantial enrichment, ranging from 2.22 to 4.61 with a mean Igeo of 3.45. Zn exhibited marked spatial variability (−2.25 to 3.29; mean = 0.14), with elevated values at TS46 and TS56. Overall, the CF, PLI and Igeo results consistently identify Pb, Co and Cu as the most strongly enriched metals, while Ti, Fe, Mn and Rb showed comparatively greater lithogenic control.

Table 4: Summary Statistics of Contamination Factor (CF), Geoaccumulation Index (Igeo) and Pollution Load Index (PLI)

Metal	***Mean CF ± SD***	***Range CF***	***Mean Igeo ± SD***	***Range Igeo***	***Mean PLI ± SD***	***Range PLI***
Ti	*2.56 ± 0.58*	*1.55–3.50*	*0.73 ± 0.34*	*0.05–1.22*	*4.83 ± 1.16*	*2.38–7.44*
V	*6.49 ± 1.61*	*2.89–9.00*	*2.06 ± 0.41*	*0.95–2.58*	*4.83 ± 1.16*	*2.38–7.44*
Cr	*6.29 ± 2.53*	*2.57–14.43*	*1.97 ± 0.54*	*0.78–3.27*	*4.83 ± 1.16*	*2.38–7.44*
Mn	*1.76 ± 0.54*	*0.52–2.69*	*0.15 ± 0.54*	*−1.53–0.85*	*4.83 ± 1.16*	*2.38–7.44*
Fe	*1.69 ± 0.48*	*0.67–2.54*	*0.11 ± 0.46*	*−1.16–0.76*	*4.83 ± 1.16*	*2.38–7.44*
Co	*19.86 ± 9.69*	*3.33–42.50*	*3.53 ± 0.83*	*1.15–4.82*	*4.83 ± 1.16*	*2.38–7.44*
Ni	*4.81 ± 5.69*	*0.57–24.00*	*1.03 ± 1.31*	*−1.39–4.00*	*4.83 ± 1.16*	*2.38–7.44*
Cu	*17.48 ± 5.85*	*7.00–36.67*	*3.47 ± 0.49*	*2.22–4.61*	*4.83 ± 1.16*	*2.38–7.44*
Zn	*2.70 ± 3.70*	*0.32–14.63*	*−0.01 ± 1.48*	*−2.25–3.29*	*4.83 ± 1.16*	*2.38–7.44*
Rb	*2.31 ± 0.66*	*1.22–3.89*	*0.56 ± 0.42*	*−0.30–1.37*	*4.83 ± 1.16*	*2.38–7.44*
Pb	*20.90 ± 13.12*	*9.50–67.50*	*3.60 ± 0.72*	*2.66–5.49*	*4.83 ± 1.16*	*2.38–7.44*

Pollution Load Index (composite, all 11 metals): mean 4.83, range 2.38–7.44.

3.5 Potential ecological risk and interpretation

The Potential Ecological Risk Index ranged from 199.9 (TS7) to 547.5 (TS52), with a mean of 349.3 ± 94.7 (Table 5). Twelve of the 30 samples (40%) fell within the moderate risk category (RI 150–300) and the remaining 18 (60%) within the considerable category (RI 300–600); none reached the high-risk threshold (RI ≥ 600). Cobalt, copper, lead and nickel each assigned the highest toxic-response weighting (Tr = 5) were the dominant contributors to RI, indicating that the ecological risk in the study area is driven principally by this metal group rather than by the more abundant but comparatively less toxic lithogenic elements. Thus, ecological risk was not restricted to isolated stations: all analysed locations showed at least moderate risk, and most were in the considerable category. This widespread pattern is consistent with multiple overlapping inputs across the estate rather than a single point source. The dominance of Co, Cu, Pb and Ni in the risk calculation reflects both their enrichment and their toxic-response

weighting. Every geochemically analysed station had PLI > 1, confirming that the multi-metal pollution burden was pervasive across the analysed subset rather than limited to a few isolated hotspots.

Table 5. Descriptive statistics for the Potential Ecological Risk Index (RI) for the study area (n = 30).

Statistics	Value
Minimum RI (station)	199.9 (TS7)
Maximum RI (station)	547.5 (TS52)
Mean RI ± SD	349.3 ± 94.7
Moderate risk (150–300), n (%)	12 (40%)
Considerable risk (300–600), n (%)	18 (60%)
High risk (≥ 600), n (%)	0 (0%)

3.6 Correlation and Multivariate Source Apportionment

The fine particulate material observed at TS30, together with its elevated Pb concentration, is consistent with a possible contribution from traffic- or machinery-related sources. The results are presented in Table 6.

Table 6. Pearson Correlation Matrix for χLF Magnetic Susceptibility and Heavy Metal Concentrations (n = 29)

Variable	χLF	Ti	V	Cr	Mn	Fe	Co	Ni	Cu	Zn	Rb	Pb
χLF	1.000	.427*	0.194	0.113	.558**	.584**	0.310	-0.020	0.062	0.129	0.213	0.127
Ti	.427*	1.000	.645**	-0.026	.781**	.742**	0.367	-0.292	0.129	.430*	.639**	0.029
V	0.194	.645**	1.000	-0.239	.611**	.696**	.410*	0.079	-0.035	0.064	0.323	-0.059
Cr	0.113	-0.026	-0.239	1.000	0.077	-0.122	-0.096	-0.086	0.166	0.098	-0.163	-0.103
Mn	.558**	.781**	.611**	0.077	1.000	.799**	.481*	-0.236	0.151	0.377	.640**	0.018
Fe	.584**	.742**	.696**	-0.122	.799**	1.000	.615**	0.048	0.276	.398*	.577**	0.044
Co	0.310	0.367	.410*	-0.096	.481*	.615**	1.000	-0.247	0.136	-0.041	0.257	0.181
Ni	-0.020	-0.292	0.079	-0.086	-0.236	0.048	-0.247	1.000	0.034	-0.056	-0.296	-0.245
Cu	0.062	0.129	-0.035	0.166	0.151	0.276	0.136	0.034	1.000	.432*	0.171	0.115
Zn	0.129	.430*	0.064	0.098	0.377	.398*	-0.041	-0.056	.432*	1.000	.446*	-0.009
Rb	0.213	.639**	0.323	-0.163	.640**	.577**	0.257	-0.296	0.171	.446*	1.000	0.364

Pb	0.127	0.029	-0.059	-0.103	0.018	0.044	0.181	-0.245	0.115	-0.009	0.364	1.000

Note: * Correlation is significant at the 0.05 level (2-tailed). ** Correlation is significant at the 0.01 level (2-tailed).

Pearson correlation analysis was conducted to examine the relationships between low-frequency magnetic susceptibility (χLF) and the concentrations of the analysed elements. The results showed that χLF had statistically significant positive correlations with Fe ($r = 0.584$, $p < 0.01$), Mn ($r = 0.558$, $p < 0.01$) and Ti ($r = 0.427$, $p < 0.05$). The strongest relationship was observed between χLF and Fe, followed by Mn and Ti. These significant positive relationships indicate that variations in magnetic susceptibility within the study area are closely associated with Fe-, Mn- and Ti-bearing mineral phases.

χLF also showed positive but non-significant correlations with Co ($r = 0.310$), Rb ($r = 0.213$), V ($r = 0.194$), Zn ($r = 0.129$), Pb ($r = 0.127$), Cr ($r = 0.113$) and Cu ($r = 0.062$). In contrast, Ni showed a very weak negative correlation with χLF ($r = -0.020$). These weak relationships suggest that the concentrations of these elements are not strongly controlled by the abundance of magnetic minerals and may reflect different sources or geochemical associations.

The significant relationships among several elements also provide evidence of common geochemical associations. For example, Fe was strongly and positively correlated with Mn ($r = 0.799$, $p < 0.01$), Ti ($r = 0.742$, $p < 0.01$), V ($r = 0.696$, $p < 0.01$), Co ($r = 0.615$, $p < 0.01$) and Rb ($r = 0.577$, $p < 0.01$). Similarly, Ti showed strong positive correlations with Mn ($r = 0.781$, $p < 0.01$), V ($r = 0.645$, $p < 0.01$) and Rb ($r = 0.639$, $p < 0.01$). These associations suggest a common geogenic or mineralogical influence on these elements. Conversely, the significant positive correlation between Cu and Zn ($r = 0.432$, $p < 0.05$) may indicate a common anthropogenic contribution.

Overall, the significant correlations of χLF with Fe, Mn and Ti demonstrate that magnetic susceptibility can provide a useful preliminary indicator of metal and mineral enrichment in soils around the Savannah Sugar Company. However, the weak correlations between χLF and several potentially toxic metals, particularly Pb, Cu, Ni and Zn, show that magnetic susceptibility should be used as a screening tool alongside direct geochemical analysis rather than as a substitute for elemental determination.

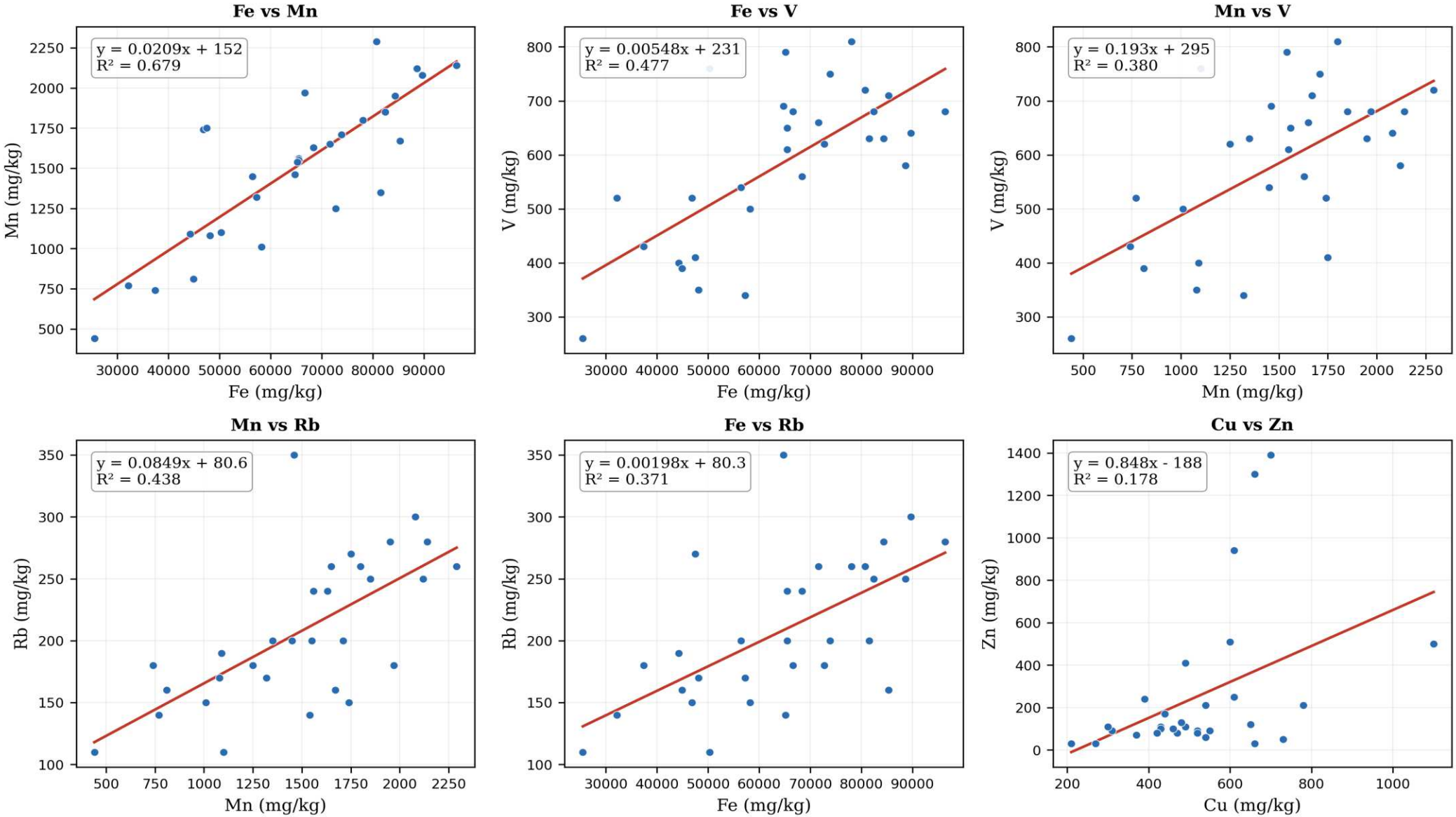


Fig. 3. Bivariate relationships among the geogenic element group (Fe, Mn, V, Rb) and between Cu and Zn, with ordinary-least-squares regression lines and coefficients of determination (R^2).

Principal component analysis retained four components explaining 70.4% of total variance (Table 6; Fig. 4). PC1 (32.7%) was dominated by Fe, Mn, V, Co and χLF, interpreted as the geogenic/pedogenic signature of the local basement complex, periodically augmented by iron-rich irrigation water. PC2 (14.5%), loaded by Cu, Zn and Cr, was interpreted as an anthropogenic agro-industrial signature linked to fertiliser/agrochemical use and industrial or waste inputs (Kabata-Pendias, 2011). PC3 (13.0%) was defined by a strong negative Pb loading and a positive Ni loading, representing two independent point sources traffic-related Pb deposition and a separate Ni input. PC4 (10.2%), loaded by Cr and χLF, was interpreted as a lithogenic Cr source tied to the magnetic mineral fraction. The separation of these components shows that contamination around the SSC reflects both natural soil-forming materials and distinct anthropogenic inputs. In particular, the Cu–Zn–Cr grouping is consistent with agro-industrial inputs, whereas the independent Pb/Ni component suggests a different source or transport pathway, potentially associated with traffic and machinery. The agreement between PCA and HCA strengthens this source interpretation, although the statistical groupings should be regarded as source indicators rather than definitive source identification.

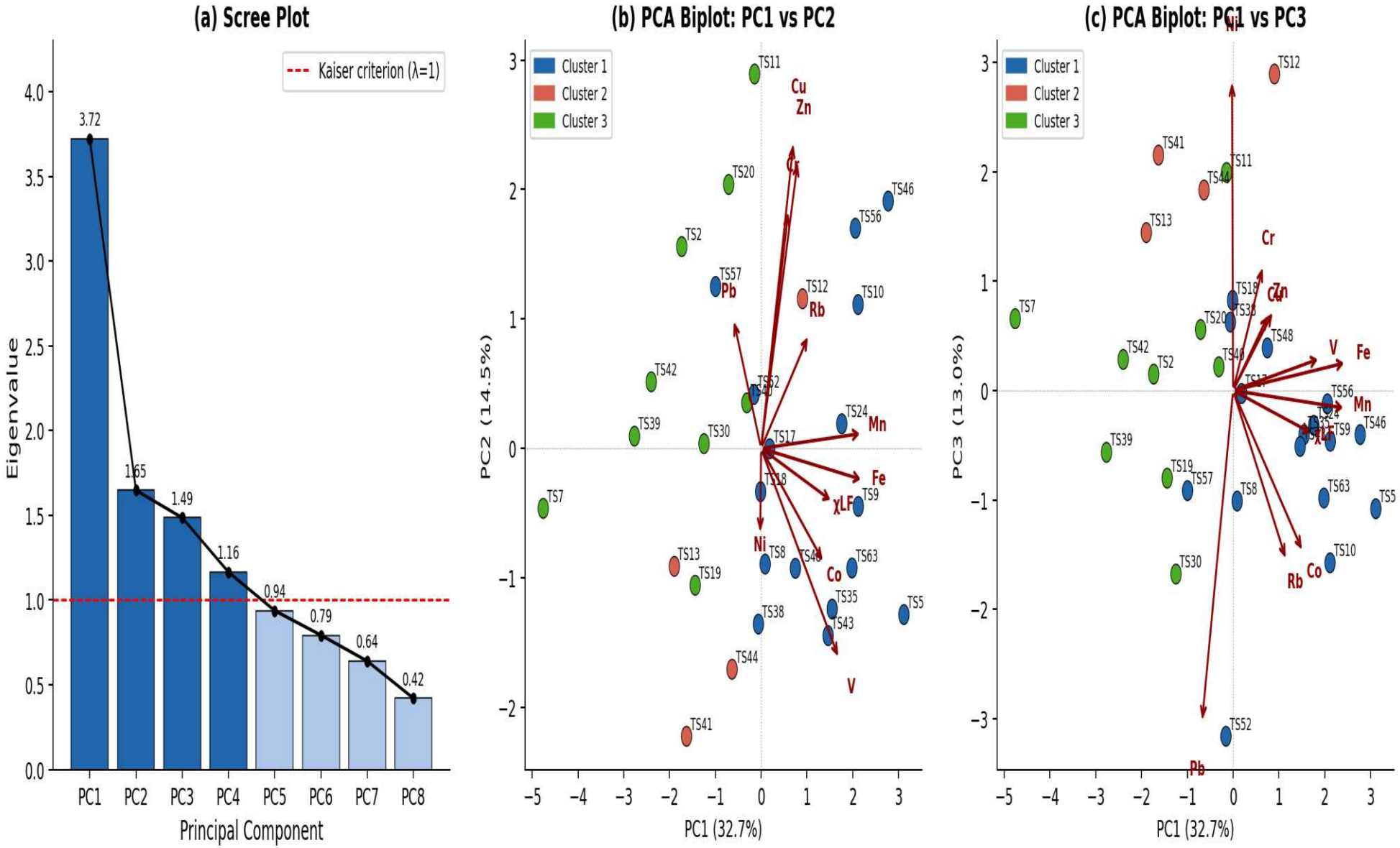


Fig. 4. (a) Scree plot of PCA eigenvalues with the Kaiser criterion (λ = 1); (b) PCA biplot of PC1 vs PC2; (c) PCA biplot of PC1 vs PC3, showing sample scores coloured by hierarchical cluster membership and element loading vectors.

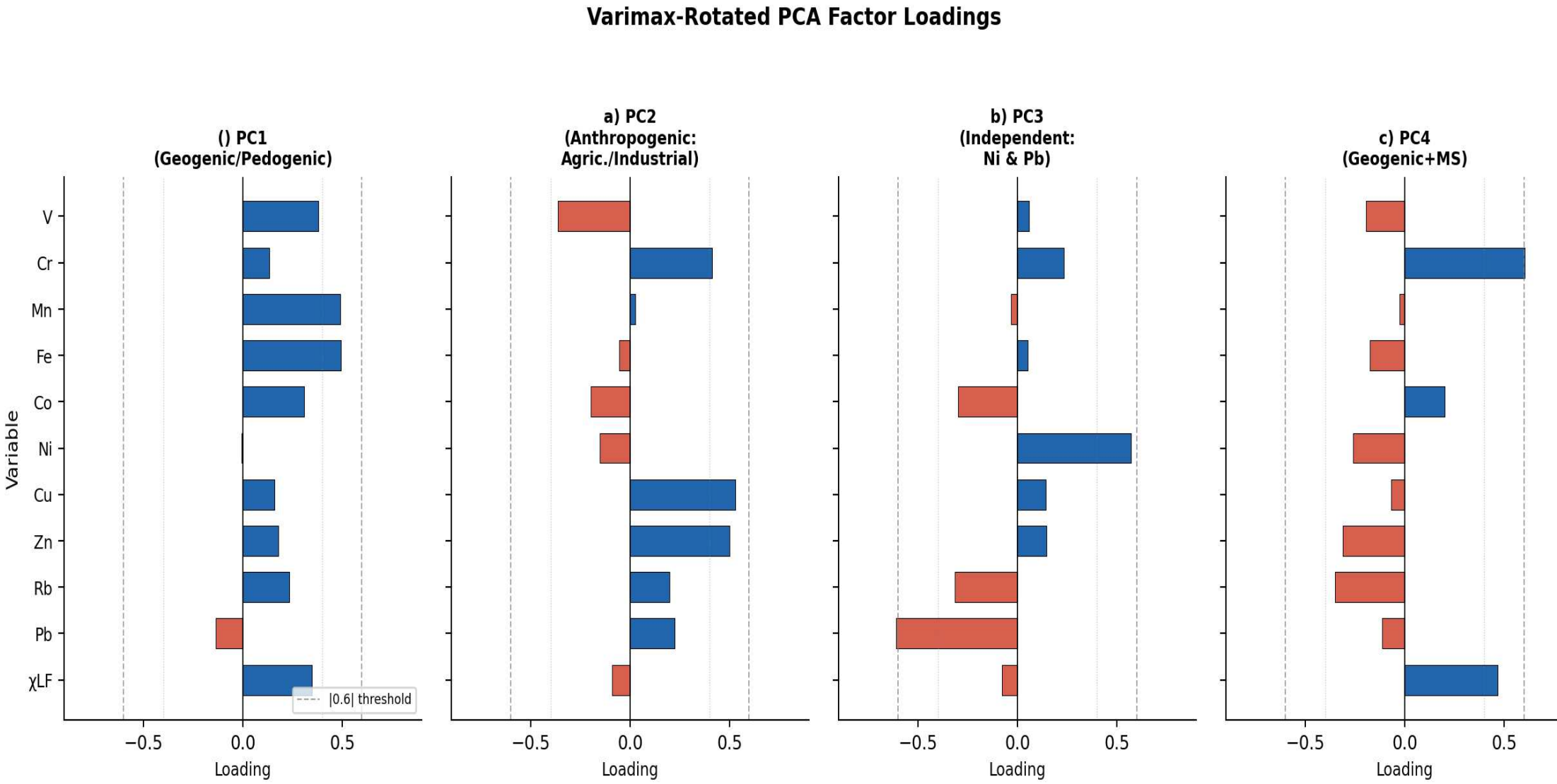


Fig. 5. Varimax-rotated factor loadings for the four retained principal components, interpreted as (PC1) geogenic/pedogenic, (PC2) anthropogenic agro-industrial, (PC3) an independent Ni/Pb source, and (PC4) a lithogenic Cr–magnetic component.

Table 7. Varimax-rotated Principal Component Analysis loadings (n = 29). Loadings of magnitude ≥ 0.40, taken as salient for interpretation, are underlined.

Variable	PC1	PC2	PC3	PC4	Communality
V	0.382	−0.364	0.059	−0.193	0.319
Cr	0.134	**0.414**	0.233	**0.604**	0.609
Mn	**0.492**	0.026	−0.032	−0.026	0.244
Fe	**0.496**	−0.054	0.051	−0.177	0.283
Co	0.308	−0.199	−0.298	0.200	0.263
Ni	−0.005	−0.152	**0.573**	−0.260	0.419
Cu	0.159	**0.531**	0.143	−0.067	0.332
Zn	0.180	**0.500**	0.148	−0.311	0.401
Rb	0.236	0.198	−0.314	−0.351	0.316
Pb	−0.137	0.226	−0.612	−0.114	0.457
χLF	0.348	−0.092	−0.079	**0.470**	0.357
Eigenvalue	3.720	1.647	1.486	1.165	—
% Variance (cumulative)	32.66	47.12	60.16	70.38	—

Hierarchical cluster analysis independently reproduced this structure, resolving three clusters (Fig. 5): a large geogenic/pedogenic cluster (n = 16), a small but distinct anthropogenic hotspot cluster with very high Ni, Cu and Zn (n = 4: TS12, TS41, TS44, TS56), and a mixed, lower-enrichment cluster (n = 9).

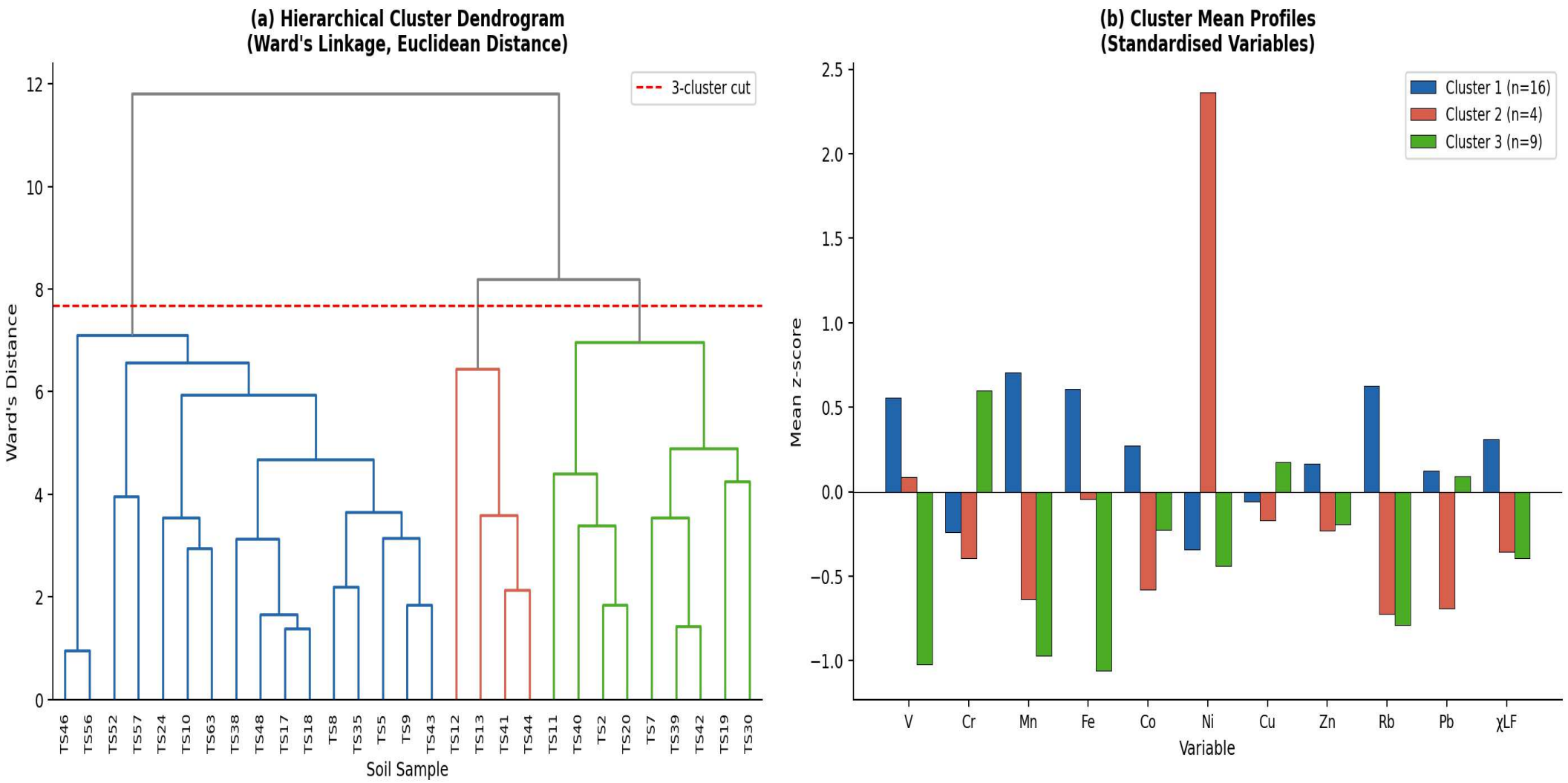


Fig. 6. (a) Ward's-linkage hierarchical cluster dendrogram of the 29 samples with matched magnetic and geochemical data, with the three-cluster solution indicated; (b) standardised (z-score) mean element profiles for each of the three clusters.

3.7 Human-health risk assessment and implications

Under mean exposure conditions, all six assessed metals returned adult Hazard Quotients below 1, with chromium the largest single contributor (HQ = 0.201), followed by lead (0.023), copper (0.018), nickel (0.012), cobalt (0.011) and zinc (0.001); the resulting adult Hazard Index (0.27) remained below the threshold of concern (Table 7). For children, however, chromium alone produced an HQ of 1.88, and the cumulative Hazard Index reached 2.43, exceeding unity and indicating a potential cumulative non-carcinogenic risk for this more vulnerable group, whose higher soil-ingestion rate relative to body weight increases per-kilogram exposure. Cancer risk from lead ingestion was estimated at 6.8×10^{-7} (adults) and 1.6×10^{-6} (children) under mean exposure, rising to 2.2×10^{-6} and 5.1×10^{-6} respectively at the maximum recorded Pb concentration (1,350 mg kg^{-1}, TS52) both above the 10^{-6} negligible-risk threshold for the most exposed individuals. Under the conservative assumption that a fraction of measured total chromium occurs as Cr(VI), the associated cancer risk (2.5×10^{-4}) substantially exceeded the acceptable 10^{-4} upper bound, identifying chromium speciation as a priority for future investigation. The contrast between adults and children reflects the greater soil intake relative to body mass assumed for children. Consequently, the child HI above unity should be interpreted as a screening-level indication of potential cumulative non-carcinogenic concern rather than evidence that adverse effects will necessarily occur. Chromium was the principal driver of the calculated non-cancer risk, while the elevated Pb concentrations remain important because of the particular vulnerability of children to lead exposure. The screening results therefore support prioritising exposure reduction for children in the more contaminated zones, while recognising that the assessment considered incidental soil ingestion and does not represent total exposure from food, water, inhalation or dermal contact.

Table 8. Mean chronic daily intake (CDI) and Hazard Quotient (HQ) for adults and children via incidental soil ingestion (n = 30).

Metal	Mean conc. (mg/kg)	Adult CDI (mg/kg/day)	Adult HQ	Child CDI (mg/kg/day)	Child HQ
Cr	440.0	6.03×10^{-4}	0.201	5.63×10^{-3}	1.875
Co	238.3	3.26×10^{-4}	0.011	3.05×10^{-3}	0.102
Ni	168.3	2.31×10^{-4}	0.012	2.15×10^{-3}	0.108
Cu	524.3	7.18×10^{-4}	0.018	6.70×10^{-3}	0.168
Zn	256.3	3.51×10^{-4}	0.001	3.28×10^{-3}	0.011
Pb	418.0	8.02×10^{-5}	0.023	7.48×10^{-4}	0.214
Total (HI)	—	—	0.265[a]	—	2.477[a]

Hazard Index (HI), the sum of the six individual Hazard Quotients.

3.8 Study limitations

Several limitations should be considered when interpreting the findings. The XRF geochemical subsample (n = 30) was smaller than the full magnetic dataset (n = 200), which constrained the statistical power of correlation and multivariate analyses. The cross-sectional sampling design provides a spatial snapshot rather than evidence of temporal trends. XRF quantified total elemental concentrations but did not determine chemical speciation or bioavailability; this is

particularly important for chromium because the health-risk calculation depends on assumptions concerning the carcinogenic Cr(VI) fraction. In addition, the health-risk assessment focused on incidental soil ingestion and therefore did not quantify total exposure through food, water, inhalation or dermal contact. These limitations do not invalidate the observed enrichment patterns, but they require cautious interpretation of source attribution and health-risk estimates.

3.9 Environmental and management implications

The findings support targeted environmental monitoring around the SSC, particularly at stations with the highest Pb, Cr, Ni, Cu and Co concentrations. Priority actions should include confirmatory laboratory analysis of identified hotspots, improved control of ash and particulate emissions, effective treatment and management of industrial wastewater and drainage, and periodic monitoring of soils used for cultivation. Community exposure-reduction measures should focus on limiting unnecessary contact with highly contaminated soil and strengthening environmental-health surveillance. Because the present assessment is screening-level, site-specific remediation or clinical interventions should be based on confirmatory environmental and public-health investigations.

4. Conclusion

This integrated assessment shows that soils around the Savannah Sugar Company, Numan, contain substantial multi-element enrichment, particularly for Pb, Co, Cu and Ni. Pollution indices indicated a pervasive multi-metal burden in the XRF-analysed samples, while most stations fell within the considerable potential ecological-risk category. Magnetic susceptibility revealed pronounced spatial and depth-related anomalies and was significantly associated with Fe, Mn and Ti in the outlier-screened correlation dataset, demonstrating value as a rapid first-pass screening tool while also showing that it cannot replace direct geochemical analysis for metals that are weakly coupled to magnetic minerals. SEM–EDS observations and multivariate analyses further indicated a mixture of geogenic/pedogenic and anthropogenic influences. The health-risk screening identified a greater potential non-carcinogenic concern for children than for adults, driven principally by chromium under the assumptions used. Overall, combining magnetic measurements with targeted XRF analysis, pollution indices and multivariate statistics provides a practical framework for identifying contaminated zones and prioritising further environmental investigation around agro-industrial facilities such as the SSC.

Declarations

Funding

This research was self-funded by the first author, Nsisong Joseph Obot. No external funding or research grants were received for this study.

Competing Interests

The authors declare that they have no competing financial or non-financial interests.

Data Availability

The datasets generated and analysed during this study are available from the author, Nsisong Joseph Obot, upon reasonable request.

Ethics Approval

Not applicable. This study involved environmental soil sampling and laboratory analysis and did not involve human participants or experimental animals.

Consent to Participate

Not applicable.

Consent for Publication

Not applicable.

Clinical Trial Number

Clinical trial number: not applicable.

References

Alengebawy, A., Khalf, B. A., Mahmoud, M., Khedr, A. H. A., Hassaan, M. S., & Elrys, A. (2021). Heavy metal and pesticide toxicity in agricultural soils and plants: Ecological risks and human health implications. Genes, 12(12), 1854.

Balali-Mood, M., Naseri, K., Tahergorabi, Z., Khazdair, M. R., & Sadeghi, M. (2021). Toxic mechanisms of five heavy metals: Mercury, lead, chromium, cadmium, and arsenic. Frontiers in Pharmacology, 12, 643972.

Das, S., Sultana, K. W., Ndhlala, A. R., Mondal, M., & Chandra, I. (2023). Heavy metal pollution in the environment and its impact on health: Exploring green technology for remediation. Environmental Health Insights, 17, 1–10.

Dearing, J. A., Dann, R. J. L., Hay, K., Lees, J. A., Loveland, P. J., Maher, B. A., & O'Grady, K. (1996). Frequency-dependent susceptibility measurements of environmental materials. Geophysical Journal International, 124(1), 228–240.

Fisher, G. L., Chang, D. P. Y., & Brummer, M. (1976). Fly ash collected from electrostatic precipitators: Microcrystalline structures and the mystery of the spheres. Science, 192(4239), 553–555.

Hakanson, L. (1980). An ecological risk index for aquatic pollution control: A sedimentological approach. Water Research, 14(8), 975–1001.

Kabata-Pendias, A. (2011). Trace elements in soils and plants (4th ed.). CRC Press.

Kanu, M., Meludu, O. C., Bassavaiah, N., & Joseph, G. (2022). Soil pollution studies of Takum, Nigeria: The use of environmental magnetic properties, elemental analysis, and geostatistical tools. Journal of African Earth Sciences (in press).

Maitera, O. N., Mustapha, A. B., Nkafamiya, I. I., & Maina, H. M. (2023). Distribution and level of heavy metals in soils and plants in the vicinity of Savannah Sugar Company, Numan, Adamawa State, Nigeria. INOSR Scientific Research, 9(3), 64–81.

Oloruntoba, A., Omoniyi, A. O., Shittu, Z. A., Ajala, R. O., & Kolawole, S. A. (2024). Heavy metal contamination in soils, water, and food in Nigeria from 2000–2019: A systematic review on methods, pollution level and policy implications. Water, Air, & Soil Pollution, 235, 586.

Orosun, M. M., Oniku, S. A., Peter, A., Orosun, R. O., Salawu, N. B., & Hitler, L. (2020). Magnetic susceptibility measurement and heavy metal pollution at an automobile station in Ilorin, North-Central Nigeria. Environmental Research Communications, 2(1), 015001.

Tchounwou, P. B., Yedjou, C. G., Patlolla, A. K., & Sutton, D. J. (2012). Heavy metals toxicity and the environment. Experientia Supplementum, 101, 133–164.

Thompson, R., & Oldfield, F. (1986). Environmental magnetism. Allen & Unwin.

Tomlinson, D. L., Wilson, J. G., Harris, C. R., & Jeffrey, D. W. (1980). Problems in the assessment of heavy-metal levels in estuaries and the formation of a pollution index. Helgoländer Meeresuntersuchungen, 33, 566–575.

United States Environmental Protection Agency (USEPA). (2011). Regional screening levels (RSLs) for chemical contaminants at superfund sites. U.S. EPA, Washington, DC.

World Health Organization / Food and Agriculture Organization (WHO/FAO). (2007). Codex Alimentarius: Joint FAO/WHO food standards programme — Codex Committee on Contaminants in Foods. WHO/FAO, Geneva/Rome.

Supplementary Files

This is a list of supplementary files associated with this preprint. Click to download.

- mainXRFElementConcentrations1dp.xlsx
- TS5.pdf
- TS35.pdf
- TS38.pdf
- TS17.pdf
- TS10.pdf
- TS46.pdf
- TS13.pdf
- TS11.pdf
- TS44.pdf
- TS19.pdf
- TS63.pdf
- TS48.pdf
- TS42.pdf
- TS86.pdf
- TS24.pdf
- TS41.pdf
- TS2.pdf
- TS56.pdf
- TS57.pdf
- TS39.pdf
- TS20.pdf
- sem0SOP.pdf
- TS8.pdf